Attenuation of Instabilities in Propulsion System Combustors

Harold T. Couch* and Leonard S. Cohen+
United Aircraft Research Laboratories, East Hartford, Conn.

A theoretical analysis of nonlinear, large-amplitude, acoustic power dissipation by screens and porous liners with and without superimposed uniform flow is presented. Screen and liner acoustic energy dissipation is described in terms of various steady flow drag coefficients which are appropriate at the large amplitudes and low frequencies characteristic of combustion instabilities in ram burners. The limiting assumption is that particle displacement is large relative to typical screen dimensions. A parallel analysis of acoustic power dissipated through a choked system exit also is derived. This analysis was utilized to estimate acoustic power production attending a large amplitude, 45-50 Hz longitudinal instability in a simulated ramjet combustor. A porous liner which incremented system dissipation by less than 5% was subsequently installed and found to be totally effective in extinguishing the observed instability.

Nomenclature

a = screen wire diameter, ft
A^* = throat area of choked exit, ft^2
c = sonic velocity, fps
C_D = screen drag coefficient
C_D° = unit screen drag coefficient, ft/sec-in.
E = energy, ft-lbf
E^* = mean sonic energy flux, ft-lbf/sec
g_c = gravitational constant = 32.174, ft-lbm/lbf-sec^2
h = static enthalpy, Btu/lbm
mwt = molecular weight, lbm/lb mol
P = pressure, lbf/ft^2
P' = instantaneous fluctuating pressure component, lbf/ft^2
P_+ = amplitude of right (downstream) traveling wave, lbf/ft^2
P_- = amplitude of left (upstream) traveling wave, lbf/ft^2
$\delta P'$ = fluctuating pressure drop across screen, lbf/ft^2
R = gas constant = 1545, lbf-ft/lb mol-°R
Re = Reynolds number
S = area (duct cross-sectional area in screen analysis), ft^2
t = time, sec
T = temperature, °R
u = flow velocity, fps
u' = instantaneous fluctuating velocity component, fps
U = volumetric flow, ft^3/sec
U' = instantaneous fluctuating volumetric flow component, ft^3/sec
w = mass flow, lbm/sec
x = axial distance in duct measured from bellmouth, ft
y = distance normal to duct wall, inches
Z = acoustic impedance, lbf-sec/ft^3
α_L = liner absorption coefficient
β = blockage factor for screen
γ = ratio of specific heats
λ = wavelength, ft
μ = viscosity, lbm/ft-sec
Π = acoustic power loss, ft-lbf/sec
ρ = density, lbm/ft^3
τ = period of oscillation, sec
ϕ_+ = phase angle of right running wave
ϕ_- = phase angle of left running wave
Φ = screen absorption coefficient
ω = angular frequency, sec^{-1}

Subscripts

e = exit
max = relative to U'_{max} in the screen/liner analysis is the maximum fluctuating velocity component at the screen/liner station
t = total (stagnation)
o = nominal or mean temporal value
1 = upstream of screen
2 = downstream of screen

Received March 12, 1973; revision received March 15, 1974.
Index categories: Aircraft Noise, Powerplant: Combustion Stability, Ignition, and Detonation.

*Supervisor, Aerothermochemistry Group, Air-Breathing Propulsion Section. Member AIAA.
+Chief, Air-Breathing Propulsion Section. Associate Fellow AIAA.

Introduction

PRESSURE fluctuations with attendant temporal velocity variations are often observed in propulsion system combustors. In ramjets and jet afterburners such instabilities, which appear to be associated with the flame-holding characteristics of the burner system, have a fundamental frequency which depends on the length of the inlet and combustor and the (average) gas temperature.[1-3] The presence of instabilities augments the intensity of turbulence within the combustor thereby increasing fuel/air mixing rates and improving the efficiency of burning. However, noise produced by the instabilities is often excessive, and the significantly increased internal heat transfer coefficients which result[4,5] place an additional burden on the enclosure thermal protection system. Accommodation of a fluctuating overpressure in a ramjet combustor also may lead to a requirement for larger inlet pressure margins which compromise achievable performance. Furthermore, the lean blowoff characteristics of the burner may be markedly perturbed so as to restrict the range of fuel-air ratios in which ramjet operation is possible.

Screech liners (composed of an array of Helmholz resonators in parallel) and quarter wave tubes have been considered for the mitigation of combustion system pressure oscillations.[6,7] Tang et al.[7] derived results pertinent to the use of a quarter wave tube for attenuation of large amplitude pressure instabilities at frequencies close to the resonant frequency of the tube. The effectiveness of quarter wave tube and Helmholz resonator devices increases as the 3/2 power of the amplitude since acoustic power is attenuated through the dissipation of flow kinetic energy.[7,8] However, unlike the quarter wave tube, the Helmholz resonator has broad band attenuation capability.[8] In general, weight and/or packaging limitations preclude the use of screech liners and quarter wave tubes in propulsion system inlet-combustion ducts where low-frequency (<500 Hz) instabilities may be encountered. By contrast, screens and absorbing liners can be simply and inexpensively integrated within engine flow passages.

The present study was motivated by the existence of a large amplitude instability in one of the research combustion facilities at UARL used to simulate a ramjet combustor. The pressure amplitude of the instability was as great as ±22 psia during operation at a mean stagnation pres-

sure of 60 psia. An absorbing liner was subsequently installed and found to be totally effective in eliminating the instability. To better understand the various system responses involved in this cure, a theoretical analysis was instigated based on the premise of Priem et al.[9] that acoustic power generated from combustion response to an existing constant amplitude instability mode must equal the sum of the losses from the exit, and all internal dissipative mechanisms.

In the analyses which follow, the "acoustic" dissipation of a screen is derived as a function of velocity amplitude and screen size subject to the assumption that the displacement amplitude is sufficiently large relative to the screen wire dimensions such that a quantitative evaluation of the operative frictional dissipation mechanisms can be obtained from the wealth of steady-state flow data. Fortunately, there are sufficient experimental data available to enable an estimate of the range of validity of this limiting assumption to be made.[10,11] The results of the screen analysis are then used to develop a procedure for computing the absorption efficiency of a porous absorbing liner by recognizing that the effect of the liner can be approximated by a series of finite-thickness elements whose flow resistance is concentrated at the geometric center of each element. The cumulative effect of these elements is then equivalent to that of a series of screens. In this analysis, absorption efficiency is related to a friction coefficient determined from steady state pressure drop versus flow velocity information for the liner material. As in the case of the screen analysis, the "acoustic" displacement amplitude must be large relative to liner pore size. This limitation is not restrictive in practice, however, since the analysis reveals that efficient porous liner design demands small pore sizes in conjuction with high void fraction.

To characterize the acoustic energy developed from the combustion process and thereby obtain an estimate of the incremental attenuation necessary to render an unstable burner system stable, the acoustic energy lost from a choked nozzle is derived. Relative to an internal acoustic energy balance, the nozzle impedance determined in this manner is that which characterizes the acoustic power dissipation as seen by internal acoustic generator, and not that which characterizes downstream acoustic power radiated at the instability frequency. In this regard, Ingard[10] in a study of the nonlinear response of an orifice, has demonstrated that large amplitude acoustic energy is nonconservative in the jet dissipation regime.

Analytical Studies

Attenuation by Screens

In what follows, the acoustic power loss, Π, resulting from the placement of a screen in a standing (or traveling) wave system is related to the screen drag coefficient and the fluctuating acoustic velocity amplitude at the screen.

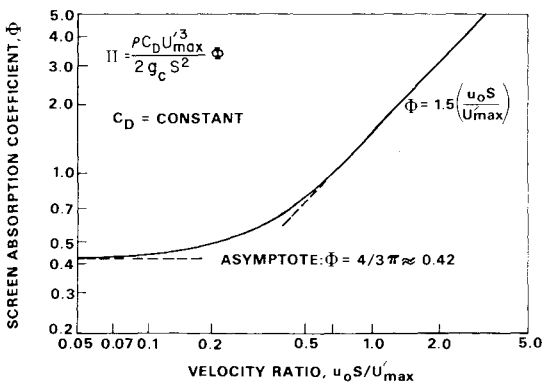

Fig. 1 Screen absorption coefficient.

The sole implicit assumption in the analysis is that the displacement amplitude is substantially greater than the characteristic screen dimension, so that steady flow drag coefficients are applicable.

In an inlet-combustor duct arrangement the local oscillatory component of the volumetric flow

$$U' = \mathbf{u}' \cdot \mathbf{S} = U'_{max} \cos\omega t \tag{1}$$

may be considered to be superimposed on a high-velocity flowfield. The volumetric flow is identical on both sides of a screen placed in the flow, i.e.,

$$U_1 = U_2 = U_0 + U'_{max} \cos\omega t \tag{2}$$

but the downstream pressure, P_2, differs from the upstream pressure, P_1, reflecting the drag of the screen

$$P_2 - P_1 = -\frac{C_D}{2g_c}\rho(u + u')|u + u'| \tag{3}$$

Thus the instantaneous rate of energy dissipation accompanying flow through the screen may be written as

$$\partial E/\partial t = -U\Delta P$$
$$= -\frac{C_D}{2g_c}\left(\frac{\rho}{S^2}\right)(u_0^2 S^2 + 2u_0 S U' + U'^2)|u_0 S + U'| \tag{4}$$

At this point it should be noted that Eqs. (3) and (4) are rigorous, and their usefulness depends only upon determining a valid mean drag coefficient, C_D. When the steady flow component, $u_0 S$ is greater than U'_{max}, Eq. (4) may be integrated in a straightforward manner (for a given variation of C_D with u') over one cycle to get the acoustic power loss. If $U'_{max} > u_0 S$, some care must be exercised in the integration in that the sign change must be accounted for when $u_0 S + U'_{max} \cos\omega t$ takes on negative values. For a constant drag coefficient, the first term obtained from the integration of Eq. (4), i.e., $\rho C_D S u_0^3/2\,g_c$ is the dissipation which occurs as a consequence of the (uniform) average flowfield. All remaining terms describe the incremental dissipation incurred as a consequence of the fluctuating velocity field, so that the acoustic power loss can be written as

$$\Pi = \frac{\rho C_D U'^3_{max}}{2g_c S^2}\,\Phi \ (C_D = \text{constant}) \tag{5}$$

where Φ is a function of the ratio of mean velocity to acoustic velocity, $u_0 S/U'_{max}$, as given in Fig. 1. When there is no steady flow component, Φ is constant ($=4/3\pi$), and acoustic dissipation is proportional to the cube of the fluctuating velocity amplitude at the screen location. This implies an acoustic resistance which is proportional to amplitude, in agreement with the experimental work of Ingard[10] for a sharp-edged orifice. As the perturbation velocity component is exceeded in magnitude by the steady-flow velocity component, the screen acts as a velocity attenuator in that acoustic power dissipation is proportional to the incident wave kinetic energy, $\rho U'^2_{max}/2g_c S$; this implies an acoustic resistance which is independent of acoustic amplitude, but which is proportional to mean flow velocity. Thus, the screen is most effective when it is located at a velocity antinode (pressure node) of the wave system in the duct.

Equation (4) also was integrated assuming the drag coefficient varies inversely with the local velocity, u', which is descriptive of a laminar dissipative process. (The utility of this assumption will be demonstrated later.) For this case, Φ is asymptotic to a value of 0.50 rather than $4/3\pi$ for vanishing mean flow velocity.

To utilize Eq. (5) requires information on the drag coefficient for the screen and a knowledge of the characteristic waveform in the duct with the screen installed. The drag coefficient may be approximated by using known drag coefficient information for cylinders, $C_{D(cyl)}$[11] modified by a function of the screen blockage factor, β. That is, the over-all drag coefficient of the screen may be written as

$$C_D = \frac{\beta}{(1-\beta)^2} C_{D(\text{cyl})} \tag{6}$$

where β is the blocked fraction of the screened area which feels drag, and the factor $(1-\beta)^2$ accounts for the fact that the local dynamic pressure through the screen ports is greater than the approach dynamic head by the square of the ratio of total area to open screen area. In this calculation, $C_{D(\text{cyl})}$ is associated with a Reynolds number for the screen based on the screen wire diameter

$$Re = \frac{\rho u a}{\mu(1-\beta)} \tag{7}$$

In Eq. (7), a is the screen wire diameter and $u = u_0 + U'_{\max}/S$ is the approach velocity. Inclusion of the factor $(1-\beta)$ accounts for the increase of the local velocity through the screen ports over the approach velocity. Flow-through screens in inlet-combustor ducts will generally be turbulent in nature and the associated drag coefficient will be relatively independent of Reynolds number and of order unity.

The introduction of a screen attenuation device into a resonant system may substantially alter the standing wave structure. The new fluctuating flowfield can be computed by matching solutions of the one-dimensional constant-amplitude wave equation, i.e., given a resonant wave system on one side of a screen, the structure of the wave system on the other side of the screen is determined by the compatibility relations; 1) conservation of mass flow, and 2) pressure drop in phase with mass flow, from Eqs. (3) and (4). The wave structure is known at an upstream location, e.g., at an orifice plate, since the forward and backward running wave strengths, P_{1+} and P_{1-}, must be equal in the case of a hard wall, and the phase angles, ϕ_{1+} and ϕ_{1-} may be taken as zero. Local fluctuating pressure components, P', and volumetric flow components, U', may be related to the amplitudes/phase angles of right and left-running waves downstream of the screen, P_{2+}/ϕ_{2+}, and P_{2-}/ϕ_{2-}, using expressions provided in Ref. 12.

Attenuation by Acoustic Liners

The principle attenuation mechanism of a porous acoustic liner is the frictional dissipation incurred during fluid inflow and outflow in response to a driving pressure perturbation. In this section, results of the screen analysis are used to develop the attenuation of a porous acoustic liner. The basis of the approach used is to recognize that the integrated effect of the liner can be approximated by subdividing the liner into finite thickness elements whose flow resistance is concentrated at the element midpoints, and treating the series of elements as a stacked array of screens. A numerical solution for the internal flow is then obtained by matching solutions of the one-dimensional wave equation on both sides of each resistance element exactly as is required in the case of the screen analysis. The analysis should be started at the interface between the liner and a hard wall backing since the forward and backward wave strengths are equal at that location. The forward-running wave transmits acoustic energy through the liner towards the backing wall. Thus it gains strength proceeding towards the liner front surface in the calculations, while the backward-running (reflected) wave loses strength. Comparison of forward and backward wave strengths at the liner front surface leads to the absorption efficiency of the liner thickness analyzed.

In the case of a porous liner with high flow resistance adjacent to a duct wall, the internal flow associated with external pressure fluctuations will be laminar, and the drag coefficient of each liner element will vary inversely with flow Reynolds number, making the acoustic resistance of each element amplitude independent. For the purpose of the present analysis it will be assumed that

$$C_D = (C_D{}^0/u')\Delta y \tag{8}$$

where $C_D{}^0$ is the steady-flow drag coefficient of 1 in. of liner material linearly extrapolated to a flow velocity of 1 fps. The differential power dissipated by each thickness element of the liner may be written using Eq. (5) as

$$d\Pi = \frac{C_D{}^0}{4}\frac{\rho U'^2_{\max}}{g_c S}\,dy = \left[-\frac{1}{\tau}\int_0^\tau U'\delta P'\,dt\right]dy \tag{9}$$

where the limiting laminar value of $\Phi = 0.5$ has been used. In Eq. (9) the parameter $U'_{\max}$ is the velocity amplitude at each liner thickness element location. In the present study, the integration of Eq. (9) for various liner thicknesses was accomplished by approximating the liner by 1/8 in. thickness elements, and the effect of the small solid volume of the liner (i.e., approximately 3%) was ignored.

Application of the liner attenuation analysis yields the ratio of incident to reflected energy at the liner surface from which the liner absorption coefficient[12] may be computed, i.e.,

$$\alpha_L \equiv \left[\frac{P_+^2 - P_-^2}{P_+^2}\right] \text{ at liner surface} \tag{10}$$

Note that the parameter α_L will be a function of frequency and liner thickness for a given liner permeability. Computations of α_L for 1 in. and 2 in. thick liners over a range of drag coefficients at various frequencies of interest are summarized in Fig. 2. For relatively permeable liners, i.e., $C_D{}^0 \leq 1000$, at low frequencies ($\lambda \gg$ thickness), the absorption coefficient increases approximately as the square of the frequency and the cube of the thickness. With decreasing permeability (increasing $C_D{}^0$) a maximum acoustic absorptivity is ultimately reached when the flow resistance becomes so great that the driving pressure perturbation is no longer capable of sustaining flow within the greater depths of the liner. This effect accounts for the fact that a 2 in. liner with a laminar drag coefficient of $C_D{}^0 = 5 \times 10^5$ is no more effective at 45 Hz than a 1 in. thick section. It should be emphasized that the predicted amplitude independence of the absorption coefficients is a consequence of a) laminar flow within the liner, consistent with b) sufficient in-depth displacement amplitudes relative to the pore dimensions such that steady-flow drag coefficients are relevant. Typically a displacement amplitude of 10 pore diam or better will satisfy these assumptions.

The liner derivation described is strictly pertinent to normal acoustic incidence since tangential pressure gradients were not considered. However, grazing incidence absorption coefficients should not be significantly different then normal coefficients in the present study where the wavelengths involved in the instability were so large relative to liner thickness that the tangential pressure gradi-

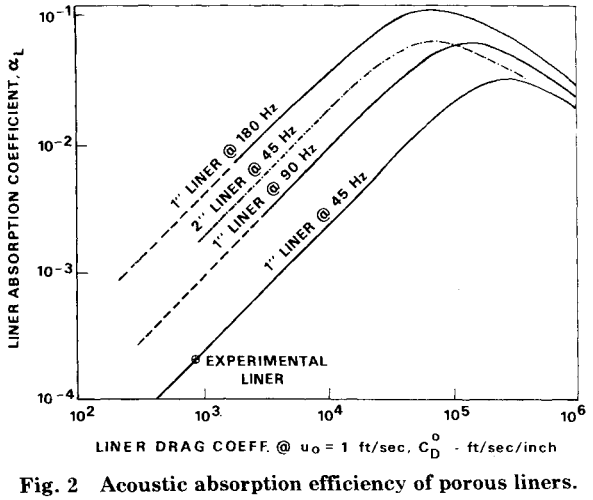

Fig. 2 Acoustic absorption efficiency of porous liners.

ent through the liner pores was negligible relative to the normal pressure gradient. Certainly, this would be so for an efficient liner ($C_D{}^0 \sim 10^5$ in Fig. 2) where the backside pressure amplitude is reduced by an order of magnitude from the frontside pressure amplitude.

It is noted that Nayfeh et al.[13] suggest that the grazing incidence absorption coefficient will be greater than the normal incidence absorption coefficient. This is partly because of crossflow through the liner pores increasing the dissipative distance through the liner as seen by a grazing wavefront, and partly because of the tangential kinetic energy loss from the acoustic mode. The latter effect is associated with the entry of fluid into the liner pores with loss of essentially all fluid tangential velocity, and subsequent reacceleration of fluid upon ejection from the liner during the following half cycle.

Choked Exit Acoustic Losses

The choked exit is by far the largest single contributor to dissipation in systems of interest in the present study. Therefore, characterization of the choked exit dissipation provides a reasonable estimate of acoustic power generation necessary for an acoustic energy balance. The total energy flux from a choked exit includes kinetic energy, chemical energy, and pressure-volume flow work. Thus, to extract the incremental flux due to an upstream acoustic instability, it is necessary to investigate the influence of an upstream pressure perturbation on jet kinetic energy, jet pressure-volume displacement, and jet temperature at the sonic point. Subsequently, the incremental dissipation relative to that without the upstream pressure perturbation can be associated with the acoustic power loss.

The instantaneous rate of energy flux through the choked nozzled is[14]:

$$\frac{dE}{dt} = w\left(h + \frac{u^2}{2g_c}\right) \tag{11}$$

Furthermore, for the flow of a perfect gas through a choked exit, where the wavelength, λ, of an upstream pressure perturbation is much greater than the nozzle characteristic dimension, the instantaneous sonic pressure, sonic temperature, and sonic velocity, can be written in terms of the mean stagnation properties assuming an adiabatic process

$$P_e/P_t = \left(\frac{2}{\gamma+1}\right)^{\gamma/(\gamma-1)}\left[1 + \frac{P'}{P_t}\cos\omega t\right] \tag{12}$$

$$T_e/T_t = \left(\frac{2}{\gamma+1}\right)\left[1 + \frac{P'}{P_t}\cos\omega t\right]^{(\gamma-1)/\gamma} \tag{13}$$

$$u_e = \left[\left(\frac{2}{\gamma+1}\right)\frac{g_c\gamma RT_t}{(mwt)}\right]^{1/2}\left[1 + \frac{P'}{P_t}\cos\omega t\right]^{(\gamma-1)/2\gamma} \tag{14}$$

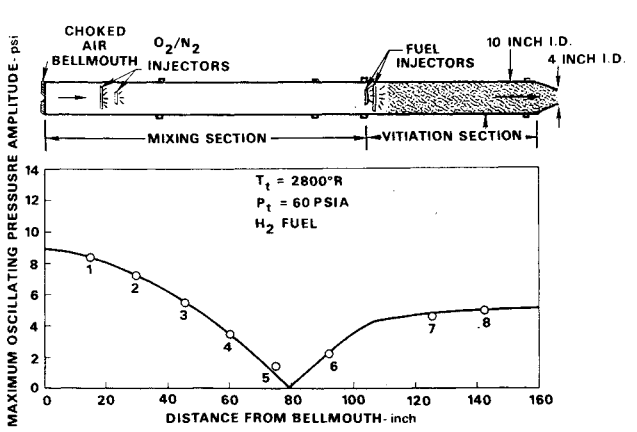

Fig. 3 Vitiation heater with typical oscillating pressure profiles.

Equation (11) may be integrated over a complete cycle after introducing the adiabatic fluid flow relationships, Eqs. (12-14), with the terms involving P'/P_t expanded in a power series, to yield the mean sonic energy flux

$$E^* = \left(\frac{2}{\gamma+1}\right)^{(\gamma+1)/2(\gamma-1)} c_t P_t A^* \left\{\frac{\gamma}{\gamma-1} + \frac{1}{8}\left(1 + \frac{\gamma-1}{2\gamma}\right)\left(\frac{P'}{P_t}\right)^2 + h.o.t.\right\} \tag{15}$$

After subtracting out the steady-state energy flux and ignoring the higher order terms, the acoustic power loss through the choked exit is obtained as:

$$\Pi^* \doteq \frac{1}{8}\left(1 + \frac{\gamma-1}{2\gamma}\right)\left(\frac{2}{\gamma+1}\right)^{[(\gamma+1)/2(\gamma-1)]} c_t A^* \frac{P'^2}{P_t} \tag{16}$$

where c_t is the sound speed based on mean total temperature, T_t, and A^* is the throat area of the choked exhaust. Note that any attenuation device which modifies the fluctuating pressure component at the choked exit also affects the acoustic power loss through the exit.

Experimental Effort

Test Apparatus

The experimental results reported in this work were obtained using the UARL vitiation heater shown in Fig. 3. The 160 in. long, 10 in. i.d. heater consists of a mixing section wherein air supplied via a (choked) bellmouth is mixed with make-up oxygen and/or nitrogen introduced through choked holes in flat-face injector rings, followed by a combustion section. Approximately 104 in. downstream of the air bellmouth, fuel is added to be mixed and burned in the 53 in. combustor (vitiation) chamber. The fuel, either hydrogen or preheated gaseous propane, also is injected through a series of choked orifices arranged on a circular flat face ring. Downstream of the vitiation section the flow passes through a conical section where the duct internal diameter is reduced to 4 in., and then through a choked exhaust nozzle.

Rig Operating Characteristics

Significant pressure fluctuation levels were observed during normal operation of the vitiation heater using either hydrogen or propane fuel at various stoichiometries, with air flow rates from 2-5 lbm/sec, and various choked exhausts. Water cooled strain gage transducers located at nine different axial stations along the vitiation heater were utilized to acquire the desired pressure data which

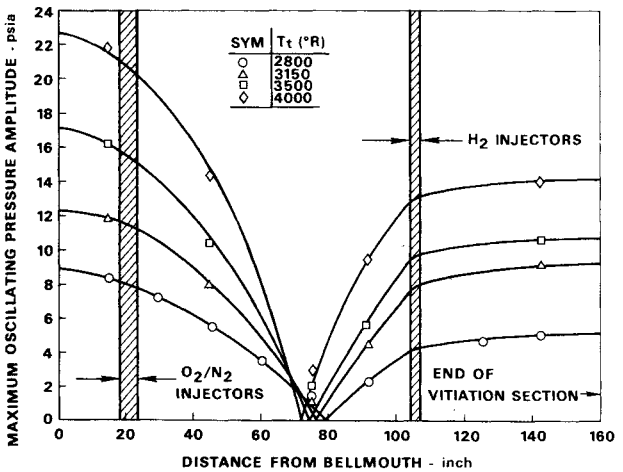

Fig. 4 Measured oscillating pressure profiles H_2/air combustion.

was recorded on magnetic tape. Typical data using hydrogen as a fuel with a choked exit area $A^* = 6.28$ in.^{2} are shown in Fig. 3. A pressure node (velocity antinode) is found approximately 78 in. from the bellmouth. A maximum pressure oscillation of 9 psi occurs at the bellmouth for operation at a lean over-all fuel-air ratio. As stoichiometric operation is approached the oscillating pressure amplitude increases, as depicted in Fig. 4. For the highest fuel/air ratio tested, i.e., $T_t = 4000$°R, the transducer nearest the bellmouth indicated a pressure of 58.2 ± 22 psia. The pressures shown in the figure are the pressure excursion amplitudes at each measurement location along the vitiation heater. Comparison of sequential readings of adjacent transducers where all transducer pressures were read out at intervals of 0.0008 sec, confirmed the existence of a standing wave resonance at the system fundamental frequency. (The term "standing wave" in the present context is used to imply nearly equal strengths of the forward and backward traveling wave components.) At each measurement location, the pressure varied sinusoidally at approximately 45 Hz, the resonant frequency, which increased only slowly with increasing combustion temperature.

In tests with propane fuel and a choked exhaust area of 4.91 in.^{2}, the oscillatory pressure amplitudes recorded at the measurement location closest to the bellmouth increased less dramatically with increases in over-all fuel/air ratio than when hydrogen was used. Recorded pressure levels were 56.2 ± 7.5 psia at $T_t = 2850$°R, 60.3 ± 8 psia at $T_t = 3350$°R, and 55.9 ± 8.5 at $T_t = 4080$°R. (Again the sequential data confirmed the existence of a fundamental standing wave resonance where the pressures varied sinusoidally at a frequency of approximately 50 Hz.)

Rig Operation With Acoustic Liner Installed

An acoustic liner composed of a 1-in. thickness of Scott Filter Foam (100 pores/in.) was formed into a 10 in. o.d. cylinder 40 in. long and installed immediately downstream of the bellmouth in the mixing section of the vitiation heater. The unit velocity drag coefficient, $C_D{}^0$, of this material determined from data provided by the manufacturer is 840 fps-in. which gives a liner absorption coefficient of 0.0002 at 45–50 Hz (see Fig. 2). This liner material in spite of its relatively modest attenuation capability was totally effective in attenuating the standing wave resonances described above where propane was used as a fuel with a test section exit area of 4.91 in.^{2}, i.e., at all fuel-air ratios tested no pressure fluctuations were found at any of the characteristic burner frequencies.

Analysis of Experimental Results

The computed first harmonic attenuation for an absorbing liner as well as the computed dissipation incurred from a 4.91 in.^{2} choked exit is given as a function of standing-wave amplitude in Fig. 5. The absorbing liner attenuation was based on a 1 in. thickness of 100 mesh filter foam lining the duct walls from the bellmouth down to 40 in. downstream of the bellmouth. The liner surface area was approximately 1200 in.^{2} and an energy absorption coefficient of 0.0002 was computed at the fundamental frequency of 45 Hz. Both screen and liner dissipations are shown as a function of the standing wave pressure potential at the bellmouth for air at 560°R and 60 psia.

The choked exit dissipation shown in the figure was computed for combustion products ($\gamma = 1.3$, $mwt = 28$) at 2880°R and 60 psia as a function of wave strength at the exit. To relate exit wave strengths to those prevailing at the bellmouth a solution of the pertinent wave equations must be obtained which satisfies the appropriate boundary conditions. A discussion of the estimated acoustic power generated as determined from an acoustic power balance at steady state will be preceeded by comments relative to the waveform analysis.

The theoretical fundamental resonant waveforms consistent with an assumed pressure amplitude of ±10 psia at the bellmouth for the original system and the system with liner are shown in Fig. 6. A double iteration is required in the calculation of the resonant waveforms since, initially, neither the resonant frequency or the acoustic power generated is known. The resonant frequency is identified when the fluctuating pressure and velocity at the upstream bellmouth and the choked exit satisfy stated boundary conditions. In the case of the choked exit, at least for acoustic wavelengths much longer than the nozzle dimensions, the analysis implies that the fluctuating pressure and velocity components are in phase and, therefore, that the characteristic impedance of a choked nozzle as seen by the combustor is real and can be derived from Eq. (16), i.e., where the impedence is appropriate for the actual choked area.

$$Z \doteq 2(3\gamma - 1)\left(\frac{\gamma + 1}{2}\right)^{(\gamma+1)/2(\gamma-1)} \rho_t c_t \qquad (17)$$

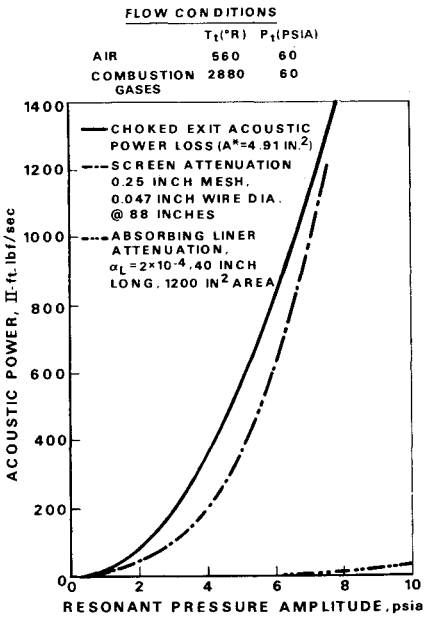

Fig. 5 Acoustic power generation and dissipation in vitiation heater.

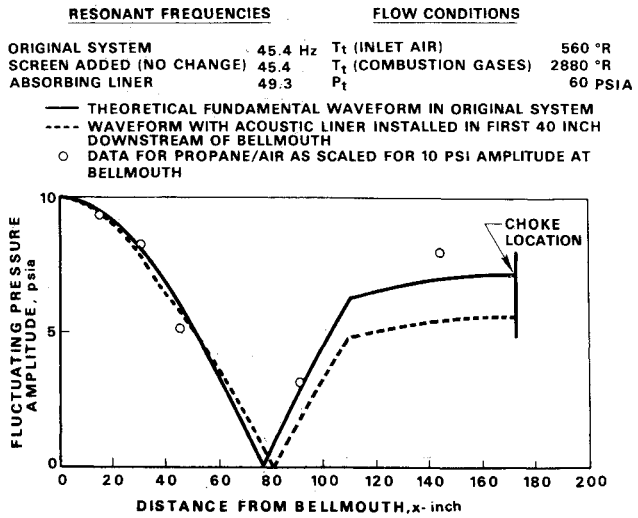

Fig. 6 Theoretical oscillatory pressure waveforms for 10 in. heater.

Table 1 Acoustic generation and dissipation in 10 in. heater

Configuration[a]	Fundamental frequency (Hz)	Acoustic attenuation[b] (ft-lbf/sec)	Amplitude choked exit[b] (psia)	Choked exit loss[b] (ft-lbf/sec)	Amplitude at burner[b] (psia)	Acoustic power available at burner[b] (ft-lbf/sec)
Original unmodified	45	–	7.2	904	6.3	904
With absorbing liner	49	31	5.6	551	4.8	<582

[a] Original unmodified system shown in Fig. 4 with 4.91 in.^{2} choked exit at x = 172 in.; fuel: propane (f/a = 0.04), inlet air mass flow = 2.7 lbm/sec, inlet temperature = 560 R, combustion temperature = 2880°R, mean pressure = 60.0 psia.
[b] Downstream pressures, dissipation, and power generated based on a fluctuating pressure amplitude of ±10 psia at the bellmouth.

In the waveform analysis, an eigen solution is obtained when the forward and backward running waves are $2n\pi$ radians out of phase at the choked exit, and when the power delivered by the volume flow generator simulating combustion response[9] is equal to the total dissipation of the system. As can be observed in Fig. 6, the eigen solution for the fundamental instability frequency reproduced the important features of the data from the original (no liner) burner system. The eigen frequency calculated was 45 Hz in comparison to the observed value of 50 Hz. The underprediction is probably a consequence of the assumption used that complete combustion is attained 110 in. from the bellmouth.

It should be observed that although the waveform analysis described can identify the acoustic field which could exist with an installed liner, it cannot answer the question of whether or not an instability would occur, or what the resonant amplitude of an instability would be. To answer this question it is necessary to know the combustion response as a function of the local oscillatory pressure and, possibly, velocity fields so that an acoustic energy balance can be made.[9] Unfortunately, existing data observed under controlled experimental circumstances are insufficient to permit a rational correlation of combustion response between different systems; however, there is an abundance of data which indicate that for any given system, combustion response is very nearly amplitude independent. That is, considering the combustion response as a negative impedance, the acoustic power generated rises as the square of the oscillatory amplitude. On the other hand from a phenomenological viewpoint combustion response must decrease with amplitude or at least not increase as rapidly with amplitude as system dissipation, or a reproducible constant amplitude resonance could not exist. Therefore, it is anticipated that a relatively small increase in system dissipation would render an unstable system stable, provided the acoustic environment in the combustion zone was unchanged.

Finally, according to the calculated results in Fig. 6, it is seen that the absorbing liner not only absorbs acoustic energy from the system, but also changes the resonant waveform (and frequency). Thus, although the attenuation is modest, a secondary benefit of the liner could be that it reduces the oscillatory pressure amplitude in the combustion zone upon which the instability must feed.

Table 1 contains computed fundamental waveform frequencies, screen and liner acoustic attenuations, choked exit losses, and by difference, estimated combustion responses, for 1) the unmodified system and 2) the system with liner installed, for an instability characterized by a ±10 psia pressure amplitude at the bellmouth. A liner may produce beneficial results by favorably modifying the instability waveform in the combustion zone in addition to its attenuation capability.

Summary and Conclusions

The analytical results demonstrate that a large amplitude longitudinal instability can be damped with a relatively small addition to system dissipation. The analysis predicts that attenuation by absorbing liners increases as the square of oscillatory pressure amplitude. In general, at low frequencies, liners are less effective attenuators, although the analysis indicates that much greater liner absorption efficiency is theoretically obtainable than presently realized through thoughtful liner design. The analytical results while unconfirmed by experiment, are limited only by uncertainty in the characterizing drag coefficients used in the study.

An analysis of acoustic power loss through a nozzle exit was derived and used to approximate an acoustic energy balance in an unstable experimental system. An absorbing liner whose attenuation represented less than 5% of total dissipation was subsequently installed and found totally effective in extinguishing a large-amplitude instability. It seems possible that the liner's effectiveness may derive partly from forcing a new pressure-velocity waveform which is less advantageous for augmentation in the flame zone.

References

[1]Tsuji, H. and Takeno, T., "Studies of High Frequency Combustion Oscillations in a Gaseous Propellant Rocket Motor," Rept. 391, March 1964, Aerospace Research Institute, Univ. of Tokyo, Tokyo, Japan.

[2]Tsuji, H. and Takeno, T., "An Experimental Investigation on High-Frequency Combustion Oscillations," *Tenth International Combustion Symposium,* Combustion Institute, Pittsburgh, Pa., 1965, pp. 1327–1335.

[3]Takeno, T., "Experimental Studies on Driving Mechanism of the High Frequency Combustion Oscillation in a Premixed Gas Rocket," Rept. 420, Jan. 1968, Aerospace Research Institute, Univ. of Tokyo, Tokyo, Japan.

[4]Hanby, V. I., "Convective Heat Transfer in a Gas-Fixed Pulsating Combustor, *"ASME Transactions, Journal of Engineering for Power,* Vol. 91, No. 1, Jan 1969, pp. 48–52.

[5]Perry, E. H. and Culick, F. E. C. "Measurements of Heat Transfer in the Presence of Large Amplitude Combustion—Driven Oscillations," to be published.

[6]Blackman, A. W., "Studies of Screeching Combustion and Pressure-wave Flamefront Interaction" *Combustion and Flame,* Vol. 5, No. 2, June 1961, pp. 175–190.

[7]Tang, P. K. and Sirignano, W. A. "Theoretical Studies of a Quarter Wave Tube," AIAA Paper 71-87, New York, 1971.

[8]Tonon, T. S. and Sirignano, W. A. "The Nonlinearity of Acoustic Liners with Flow Effects," AIAA Paper 70-128, New York, 1970.

[9]Priem, R. J. and Rice, E. J. "Combustion Instability with Finite Mach Number Flow and Acoustic Liners," *Twelfth International Combustion Symposium,* Combustion Institute, Pittsburgh, Pa., 1969, pp. 149–159.

[10]Ingard, U. and Ising, H., "Acoustic Nonlinearity of an Orifice," *Journal of the Acoustic Society of America,* Vol. 42, No. 1, 1967, pp. 6–17.

[11]Schlichting, H., *Boundary Layer Theory,* 4th ed., McGraw-Hill, New York, 1960.

[12]Beranek, L. L., *Acoustics,* McGraw Hill, New York, 1954.

[13]Nayfeh, A. N. and Sun, J. "Effect of Transverse Velocity and Temperature Gradients on Sound Attenuation in Rectangular Ducts," VPI Tech. Rept. VPI-73-24, Sept. 1973, Virginia Polytechnic Inst., Blacksburg, Va.

[14]Sage, B. H., *Thermodynamics of Multicomponent Systems,* Reinhold, New York, 1965.